PROCEEDINGS B

royalsocietypublishing.org/journal/rspb

Research

Cite this article: Ghedini G, Malerba ME, Marshall DJ. 2020 How to estimate community energy flux? A comparison of approaches reveals that size-abundance trade-offs alter the scaling of community energy flux. *Proc. R. Soc. B* **287**: 20200995.
http://dx.doi.org/10.1098/rspb.2020.0995

Received: 4 May 2020
Accepted: 26 June 2020

Subject Category:
Ecology

Subject Areas:
ecology

Keywords:
competition, homeostasis, metabolism, phenotype, species interactions, stability

Author for correspondence:
Giulia Ghedini
e-mail: giulia.ghedini@monash.edu

Electronic supplementary material is available online at https://doi.org/10.6084/m9.figshare.c.5082856.

THE ROYAL SOCIETY PUBLISHING

How to estimate community energy flux? A comparison of approaches reveals that size-abundance trade-offs alter the scaling of community energy flux

Giulia Ghedini, Martino E. Malerba and Dustin J. Marshall

Centre for Geometric Biology, School of Biological Sciences, Monash University, Melbourne VIC 3800, Australia

GG, 0000-0002-5156-2009; MEM, 0000-0002-7480-4779; DJM, 0000-0001-6651-6219

Size and metabolism are highly correlated, so that community energy flux might be predicted from size distributions alone. However, the accuracy of predictions based on interspecific energy–size relationships relative to approaches not based on size distributions is unknown. We compare six approaches to predict energy flux in phytoplankton communities across succession: assuming a constant energy use among species (per cell or unit biomass), using energy–size interspecific scaling relationships and species-specific rates (both with or without accounting for density effects). Except for the per cell approach, all others explained some variation in energy flux but their accuracy varied considerably. Surprisingly, the best approach overall was based on mean biomass-specific rates, followed by the most complex (species-specific rates with density). We show that biomass-specific rates alone predict community energy flux because the allometric scaling of energy use with size measured for species in isolation does not reflect the isometric scaling of these species in communities. We also find energy equivalence throughout succession, even when communities are not at carrying capacity. Finally, we discuss that species assembly can alter energy–size relationships, and that metabolic suppression in response to density might drive the allometry of community energy flux as biomass accumulates.

1. Background

The allometry of energy–size relationships (scaling exponent less than 1) and their regularity among species suggests that the size distribution of organisms affects community energy flux [1]: that is, communities composed of smaller individuals should have higher mass-specific rates than communities of larger individuals [2,3]. Scaling relationships that quantify how energy use varies across sizes (and species) could thus predict community energy flux solely based on size distributions [4,5]—providing a powerful tool to estimate function, because size distributions are generally easier to obtain than measures of whole community function. Furthermore, interspecific scaling relationships could inform on how changes in size driven by anthropogenic pressures (e.g. exploitation, warming) affect the transfer of energy in ecological systems [6,7]. The reliability of these predictions, however, depends on whether interspecific patterns of energy use based on size adequately approximate community function [8].

While interspecific scaling relationships based on size predict large-scale ecological patterns [9–11], their predictive power decreases at smaller scales [12–16]. Hence, size alone might not be the most informative variable of energy flux in populations and communities, but this remains an open question. Few studies have tested the ability of interspecific scaling relationships to predict empirical patterns of community energy flux, and even fewer their relative merit in comparison to alternative approaches (e.g. not based on size structure or including more species-specific information) [17] but see [18,19].

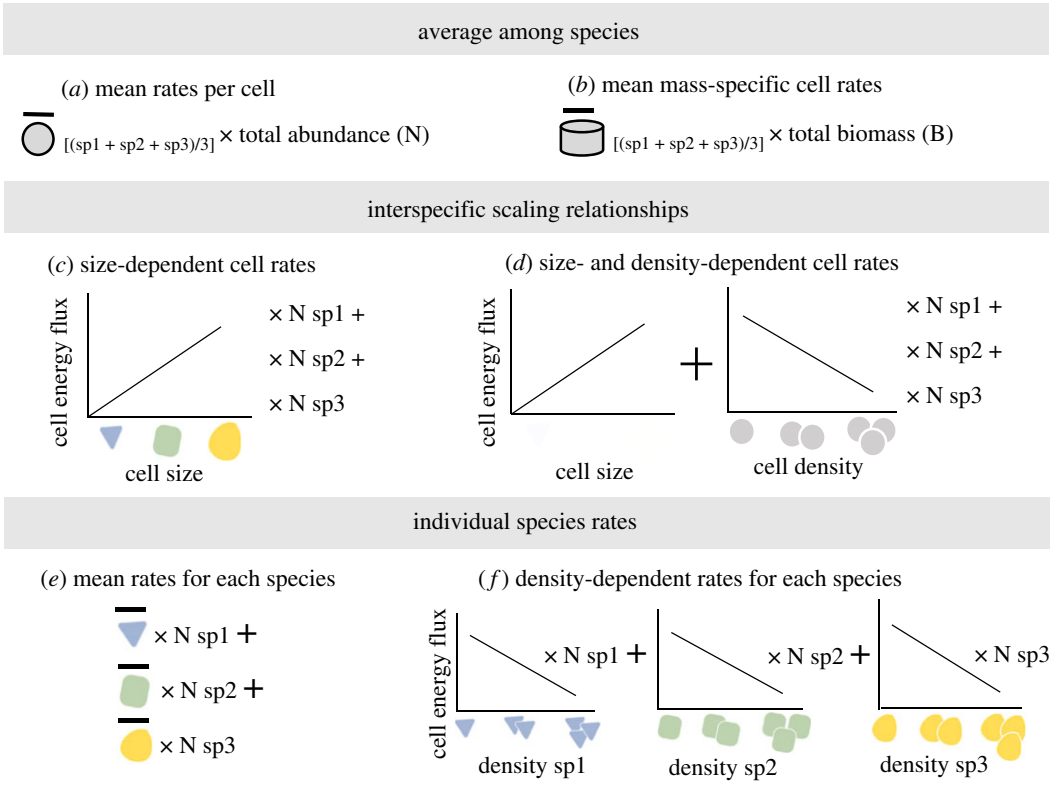

Figure 1. Schematic of the approaches used to estimate energy flux in phytoplankton communities (example with a 3-species community): from the average among species of (*a*) per cell energy use or (*b*) biomass (biovolume)-specific rates; interspecific scaling relationships that account for the (*c*) size- or (*d*) size and density dependence of cell energy use; individual species rates of (*e*) mean cell energy use or (*f*) density-dependent cell energy use. (Online version in colour.)

Of the studies that have formally tested predictions of interspecific scaling relationships, some found good agreement between predictions and data [3,20,21], while others found deviations from expected patterns [2,7,8,22]. Some of these inconsistencies could be due to the use of general size scaling exponents (e.g. ¾). Since the allometry of energy use varies among groups of organisms [23–25], taxon-specific exponents can improve the reliability of predictions based on interspecific scaling relationships [19,21,26]. Accounting for density-dependent energy use could further improve predictions [27–29], but to the best of our knowledge, this approach has yet to be tested.

While size is a good predictor of individual metabolism, community energy flux can be insensitive to size structure. For instance, when metabolism scales isometrically with mass, as for many unicellular organisms [29–31] particularly when estimated as a function of carbon content [32]. Under isometry, biomass-specific energy use is equivalent for small and large organisms. The influence of size structure on energy flux might also disappear when communities are at carrying capacity as predicted by the energy equivalence rule [2,33]. Under energy equivalence, the total energy flux per unit area is invariant of size because the higher metabolism of larger organisms is perfectly compensated for by their lower abundance, i.e. reciprocal scaling of density and metabolism with size [21,34]. The value of the scaling exponent then determines how energy flux varies as a function of biomass: under hypoallometry biomass-specific energy flux declines for larger species [2], while under isometry it is constant [31].

We compare the relative ability of six approaches of increasing complexity to predict energy flux in phytoplankton communities during succession under two light environments. Each approach underlies specific hypotheses about the processes that drive community energy flux and, therefore, requires different amounts of information (figure 1). The approaches and their assumptions are formalized and described in detail in the Methods section. Since energy intake and expenditure can scale differently with size or have different density dependence [27,29,32], we extend our analysis to quantifying metabolism, photosynthesis, and net energy production (their difference). The model underlying each approach was parametrized from an independent dataset where rates of energy use were measured for the phytoplankton species individually as a function of cell biovolume (μm^3, a proxy for biomass) and population density [29]. We then used information on size structure, biovolume, or abundance to estimate community energy flux and compare the relative bias, precision, and accuracy of these approaches in predicting empirical measurements of metabolism and net production.

2. Methods

(a) Empirical measurements of community energy flux

Community energy flux was measured empirically on two sets (runs) of marine phytoplankton communities with 10 replicate communities each. The two runs were set-up four weeks apart and exposed to a light intensity of 75.4 ± 3.9 µm quanta m^{-2} s^{-1} and 111.2 ± 5.4, respectively. The details of this experiment are described in [35]. Briefly, communities were established by mixing equal biovolumes of six species (4 to 500 μm^3 in size) in clear glass funnels (500 ml) kept at 22 ± 1°C. Each week for 10 weeks, we measured photosynthesis and respiration rates under seven light intensities (0–300 µm quanta m^{-2} s^{-1} at increments of 50) from five subsamples (5 ml) of each community. Oxygen

rates (µmol O_2 min^{-1}) were measured using 24-channel PreSens sensor dish readers (AS-1 Scientific Wellington, New Zealand) and calculated for each subsample as $VO_2 = -1 \times ((m_a - m_b)/100) \times V\beta O_2$, where m_a is the rate of change of O_2 saturation in each sample (min^{-1}), m_b is the mean O_2 saturation across all blanks (min^{-1}), V is the water volume (0.005 l), and βO_2 is the oxygen capacity of air-saturated seawater at 20°C and 35 ppt salinity (225 µmol O_2 l^{-1}). The rate of oxygen production or consumption was averaged among the five subsamples of each community and across light intensities. Oxygen rates were converted to calorific energy (J min^{-1}) using the conversion factor of 0.512 J (µmol O_2)$^{-1}$ [36] and calculated for the whole community (J min^{-1} for 500 ml) assuming a 16 L : 8D cycle for consistency with [29], albeit communities were grown under a 14 L : 10D cycle. Community metabolism was calculated over 24 h as the sum of 16 h of light metabolism and 8 h of dark metabolism. Community net production was calculated as 16 h of photosynthesis minus 8 h of respiration (average metabolism per hour × 8 h). For each community, we used light microscopy to determine the density (cells $µl^{-1}$) and biovolume ($µm^3$) of each species, and from these calculated species biovolumes and total community biovolume ($µm^3$ in 500 ml).

(b) Estimates of community energy flux

We used six approaches to estimate community metabolism and net production across succession (figure 1). The parameters used in each approach are derived from an independent dataset presented in Malerba *et al*. [29] where the authors quantified the scaling of cell metabolism and net production as a function of cell size (biovolume, μm^3) and population density across 21 phytoplankton species, including the same species included in the communities. Measurements were performed across six light intensities (0–250 µm quanta m^{-2} s^{-1}) and four population densities standardized by biomass density at 21 ± 2°C. Daily cell metabolism (Joules day^{-1} $cell^{-1}$) was calculated for 24 h of darkness and net production as the difference between 16 h of photosynthesis and 8 h of respiration. For consistency, all estimates of community energy flux were calculated over the same light cycle (Joules day^{-1} for a community of 500 ml). The approaches, their assumptions, and the steps taken to estimate community energy flux are described below and presented in detail in electronic supplementary material, table S1.

(i) Mean rates per cell among species

$\bar{E}_{com} = \bar{E}_{cell}\,(\bar{E}_{cell\ sp1}, \bar{E}_{cell\ sp2}, \ldots, \bar{E}_{cell\ spn}) \times N$. This approach assumes that community energy flux ($\bar{E}_{com}$) is the product of the mean individual (per cell) energy use among all species ($\bar{E}_{cell}$, given $\bar{E}_{cell\ spn}$ the individual energy use of each species) and the total abundance of organisms (N), regardless of identity or size. We calculated the per cell energy use of each species from their population rates [29] and then multiplied the grand mean among species by the total abundance of cells in communities. This approach does not consider changes in size distributions but might work if species have similar rates of energy use and if changes in the abundance of organisms are stronger drivers of energy flux than changes in size.

(ii) Mean biomass-specific cell rates among species

$\bar{E}_{com} = \bar{E}_{bio}\,(\bar{E}_{bio\ sp1}, \bar{E}_{bio\ sp2}, \ldots, \bar{E}_{bio\ spn}) \times B$. This approach requires a similar amount of information as the approach above, but focuses on biomass (or biovolume)-specific rates rather than rates per cell. It assumes that community energy flux changes proportionally (isometrically) to community mass. Community energy flux can thus be predicted from the mean biomass-specific energy flux among species ($\bar{E}_{bio}$, with $\bar{E}_{bio\ spn}$ the biomass-specific cell energy use of each species) and total mass (B). In our phytoplankton species, cell energy use scales hypoallometrically with cell biovolume ($µm^3$ used as a proxy for mass) at constant density [29]. However, isometry between community energy flux and mass can emerge even when metabolism scales allometrically for individual species [26]. Therefore, this approach could work even for communities of species for which metabolism scales allometrically when measured in isolation. We used the independent dataset to calculate the biovolume-specific energy use for each species by dividing their cell rate (calculated above) by their average cell biovolume; we then multiplied the overall mean biovolume-specific rate by total community biovolume.

(iii) Size-dependent cell rates across species

$\bar{E}_{com} = \sum_{i=1}^{s} (\bar{E}_{cell i} \times N_i)$, where $\log_{10}(\bar{E}_{cell i}) = \alpha + \beta \times \log_{10}(\bar{S}_i)$. This approach assumes that community energy flux can be predicted from size distributions because energy use is highly correlated with size. On a log-scale, these scaling relationships quantify the common size dependence (β) of cell energy use and its intercept (α) across species within a taxon. Hence, the average cell energy use ($\bar{E}_{cell i}$) of any species within that taxon can be predicted from these common parameters based on the species' average size ($\bar{S}_i$). Total community energy flux is the sum across species of cell rates, converted to arithmetic scale, multiplied by the abundance of each species within the community (N_i). We used the interspecific scaling functions (2.1) and (2.2) below [29] to estimate cell metabolism and net production for each species as a function of their average biovolume ($µm^3$) in the community and then calculated total community energy flux by adding the contribution of each species based on their abundance.

$$\log_{10}(\text{cell metabolism J d}^{-1}\ \text{cell}^{-1}) = 0.71 \times \log_{10}(\text{mean cell volume}) - 7.32 \quad (2.1)$$

$$\log_{10}(\text{cell net production J d}^{-1}\ \text{cell}^{-1}) = 0.63 \times \log_{10}(\text{mean cell volume}) - 6.89 \quad (2.2)$$

(iv) Size- and density-dependent cell rates across species

$\bar{E}_{com} = \sum_{i=1}^{s} (\bar{E}_{cell i} \times N_i)$, where $\log_{10}(\bar{E}_{cell i}) = \alpha + \beta \times \log_{10}(\bar{S}i) + \delta \times D_i$. This approach is similar to the above with the difference that it also estimates the common density dependence of cell energy use across species (δ) as a function of their population biomass density (D_i) [29]. We used the full interspecific scaling functions from [29] to estimate cell metabolism (2.3) and net production (2.4) based on size and density:

$$\log_{10}(\text{cell metabolism J d}^{-1}\ \text{cell}^{-1}) = 0.71 \times \log_{10}(\text{mean cell volume}) - 0.004 \times \text{concentration} - 7.32 \quad (2.3)$$

$$\log_{10}(\text{cell net production J d}^{-1}\ \text{cell}^{-1}) = 0.63 \times \log_{10}(\text{mean cell volume}) - 0.004 \times \text{concentration} - 6.89, \quad (2.4)$$

where concentration is the population density expressed as biomass concentration (equivalent to optical density, reported in %), which allows better comparison than cell number given differences in size among species. We calculated cell rates in two ways: (i) from the species population density which assumes that cell energy use is density dependent only in response to conspecifics and (ii) from total community density, thus assuming that each cell is affected equally by all other cells independently of species.

(v) Average individual species cell rates

$\bar{E}_{com} = \sum_{k=1}^{s} ((\bar{E}_{cell\ sp1} \times N_{sp1}) + (\bar{E}_{cell\ sp2} \times N_{sp2}) + \ldots + (\bar{E}_{cell\ sp1} \times N_{sp\,s}))$. This approach assumes that differences in energy use

among species are important and therefore energy use needs to be measured for individual species [19,21,26], but it also assumes that the effect of density can be ignored. Community energy flux is the sum across species of the average cell energy use of each species ($\bar{E}_{\text{cell sps}}$; calculated for the first approach without averaging across all species) multiplied by its abundance (N_{sps}).

(vi) Density-dependent individual species cell rates

$\bar{E}_{com} = \sum_{k=1}^{s} (\bar{E}_{\text{cell spk}} \times N_{spk})$, where $\log_{10}(\bar{E}_{\text{cell spk}}) = \alpha_k + \delta_k \times \log_{10}(D_k)$. This last approach accounts for species-specific differences in metabolic density dependence, so that the cell energy use of each species ($\bar{E}_{\text{cell spk}}$) is calculated as a function of its population biomass density (D_k) using species-specific parameters (δ_k, α_k). This approach should perform better than all others given that it includes the most information; the obvious drawback is that it requires much more data. From the independent dataset [29], we estimated the decline in cell metabolism and photosynthesis with increasing biomass density for each species using linear models on $\log_{10}$-transformed data (electronic supplementary material, table S1, figure S1). We used these species-specific parameters to calculate the cell rates of each species from (i) its population density (i.e. only intraspecific competition) or (ii) the community biomass density (i.e. interspecific effects equal to intraspecific effects). In both cases, community rates are the sum of population rates (cell rates × abundance of each species).

(c) Statistical analyses

We tested the ability of each approach to predict changes in community energy flux using linear mixed models on untransformed data, including the community as a random effect and using Wald tests to calculate 95% confidence intervals. The relative performance of the approaches was evaluated based on precision, bias, and accuracy. Precision was measured by the R^2 of the regressions—a low precision (low R^2) indicates that the estimates are spread out relative to each other (high variance). Bias was calculated as the difference between 1 (all data points fall on a straight line) and the observed slope [37]. Positive bias indicates that the estimator overestimates the true value of community energy flux (regression slope less than 1), while negative bias that it underestimates it (regression slope greater than 1) [38]. We calculated the mean square error (MSE) as a measure of accuracy, which is defined by the combination of both bias and precision and indicates how close the estimator is to the true value [39]. The MSE was calculated across all 100 values of community energy flux within each run (n) as $\text{MSE} = 1/n \times \sum_{i=1}^{n} (Yi - \hat{Y}i)^2$ where Y_i is each estimate of community metabolism (or net production) and $\widehat{Y}i$ is the actual (observed) value. For each approach, we report the squared root of the MSE (RMSE), which has the same unit as community energy flux (J d^{-1}), standardized by the approach with lowest RMSE within that run for easier comparison. Therefore, an RMSE of 1 identifies the best approach and values greater than 1 progressively worse approaches.

We used linear models to estimate the relationship between (i) cell density and population biomass concentration and (ii) the density dependence of cell energy use for each species (electronic supplementary material, table S1, figure S1). Data of cell density, metabolism, and photosynthesis were $\log_{10}$-transformed prior to analyses to meet assumptions of normality and homogeneity of variance. For all analyses, these assumptions were assessed visually by plotting residuals versus fitted values and Q-Q plot, respectively. To test for energy equivalence, we used linear mixed models between (i) total cell abundance and average cell size among all species, (ii) average cell metabolism (net production) and average cell size, (iii) community metabolism (net production) and average cell size, and (iv) community metabolism (net production) and total biovolume. The community was included as a random effect and data were $\log_{10}$-transformed prior to analyses. Data collected on the first sampling time (week 0) were removed because abundance and size were experimentally manipulated (to achieve equal biovolumes among species) and therefore could not be used to assess size-abundance trade-offs. Statistics and plots were performed in RStudio Team (2015) using packages *lme4* [39], *lmerTest* [40], *car* [41].

3. Results

Overall, each approach performed quite consistently in its ability to predict community metabolism and net production (figure 2), so that we were able to rank them based on their average accuracy (electronic supplementary material, table S2). Rates reconstructed from the mean energy use per cell (first approach), performed substantially worse than all others (average RMSE = 34.8 ± 4.13). Conversely, the similarly simplistic approach based on mean biomass-specific rates was the most accurate overall and the most consistent (RMSE = 1.03 ± 0.02). It was the approach that best-predicted community metabolism (figure 2, see electronic supplementary material, figure S2 for separate runs), while net production was best predicted by individual species rates with density effects (figure 2, electronic supplementary material, figure S3).

Most approaches had positive bias with high intercepts (electronic supplementary material, table S3), therefore they underestimated community energy flux at low values and overestimated them at larger values (figure 2 except k). The most complex approach (density-dependent individual species rates) had generally lower bias and intercepts. This approach ranked second for overall accuracy when cell rates were calculated from species densities (RMSE = 1.12 ± 0.11), and third when calculated from community density (1.26 ± 0.04). Estimates based on interspecific scaling relationship with density dependence ranked fourth when calculated from species densities (1.34 ± 0.15). Accounting for density-dependent energy use, either across or within species, typically lowered intercepts and increased accuracy (figure 2; electronic supplementary material, table S3). Model predictions overestimated community energy flux when calculated assuming only intraspecific competition, while they underestimated it when based on total community density (electronic supplementary material, figures S4 and S5).

Precision was variable and always below 0.7 indicating that at least 30% of community energy flux was influenced by factors that we have not accounted for. All approaches had larger errors (lower accuracy) for larger values of community energy flux (electronic supplementary material, figure S6), with the exception of the worst approach (mean rates per cell) for which accuracy improved for larger values of energy flux. The most complex approach (density-dependent individual species rates) also showed this pattern for metabolism (electronic supplementary material, figure S6).

(a) Community metabolism

(i) Mean rates per cell

Assuming a constant energy use per cell among all species grossly overestimated community metabolism (figure 2*a*). This approach suffered from the lowest precision ($R^2 = 0.004$

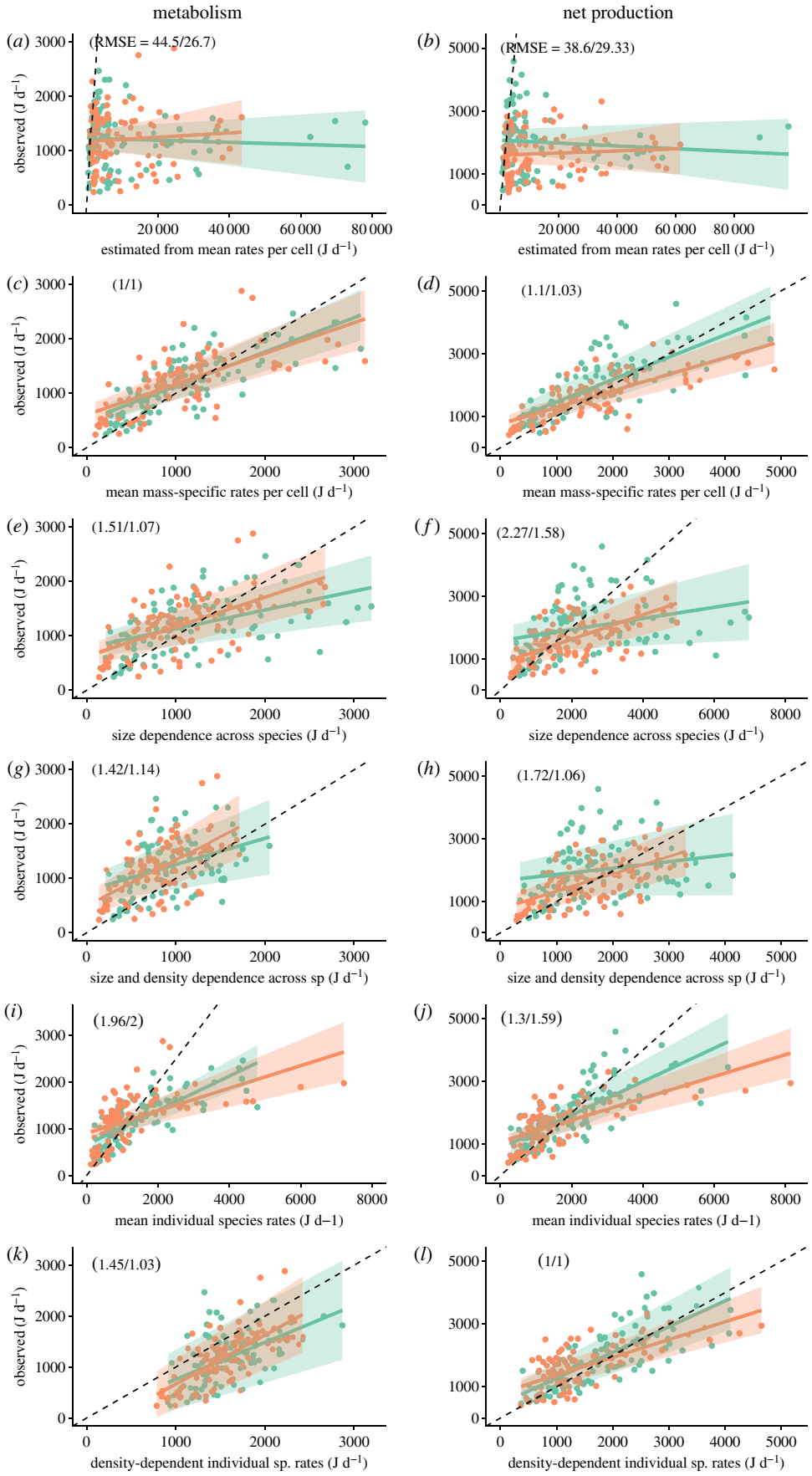

Figure 2. Relationship between observed community metabolism (left) or net production (right) and estimates of community rates from each approach: mean rates per cell (*a*,*b*), mean cell mass-specific rates (*c*,*d*), size-dependent cell energy use across species (*e*,*f*), size- and density-dependent cell energy use across species (*g*, *h*), mean cell rates for individual species (*i*,*j*), and density-dependent cell rates for individual species (*k*,*l*). Each graph reports the square root of the mean square error (RMSE) for run 1 (left; green) and run 2 (right; orange) with 1 indicating the most accurate approach and values greater than 1 progressively lower accuracy. Only estimates from species density are shown (electronic supplementary material, figures S4 and S5 for community density). Each point represents a community at each sampling time. Solid lines are mean estimates from linear mixed models with 95% Wald confidence intervals. Broken lines represent the 1 : 1 line. (Online version in colour.)

and 0.006), greatest bias (approx. 1), and lowest accuracy (RMSE approx. 30 times greater than other approaches, electronic supplementary material, table S3).

(ii) Mean biomass-specific rates per cell

Despite not including more information than the approach above, mean biomass-specific cell rates predicted community metabolism with the greatest accuracy (RMSE = 1; electronic supplementary material, table S1, figure 2*c*). This approach ranked third for precision (R^2 = 0.57 and 0.44, electronic supplementary material, table S3) and had positive bias (0.37 and 0.44; electronic supplementary material, figure S6).

(iii) Size-dependent cell rates across species

Conversely, predictions from the interspecific scaling of cell metabolism with cell size had lower precision (R^2 = 0.22 and 0.37) and higher positive bias (0.66 and 0.46, electronic supplementary material, table S3). It also had lower accuracy but this was more run-dependent as it performed substantially better in run 2 (RMSE = 1.51 and 1.07, figure 2*e*).

(iv) Size- and density-dependent cell rates across species

Accounting for the effects of both size and density on cell metabolism across species improved accuracy for run 1 but decreased it for run 2 (RMSE = 1.42 and 1.14; figure 2*g*). Precision (R^2 = 0.15 and 0.36) and bias (0.52 and 0.15) were also worse in run 1 compared to run 2 (electronic supplementary material, table S3). Estimates were more accurate when built on species densities than community density (electronic supplementary material, figure S4).

(v) Average individual species cell rates

The average energy use of individual species was a poor predictor of community metabolism: accuracy was low (RMSE = 1.92 and 2) largely overestimating community metabolism for some communities (figure 2*i*). This approach had good precision (R^2 = 0.61) but high bias (0.64) in run 1 and low precision (R^2 = 0.31) and high bias in run 2 (0.76, electronic supplementary material, table S3).

(vi) Density-dependent individual species cell rates

When accounting for density dependence, the metabolic rates of individual species led to much better estimates of community metabolism (figure 2*k*). In run 1, predictions were more accurate when based on community density (RMSE = 1.26) than species density (RMSE = 1.45), but in run 2, we found the opposite pattern (electronic supplementary material, table S2). Overall, bias was lowest when estimates were based on species densities (0.27 and 0.04), while precision was highest when based on community density (R^2 = 0.69 and 0.52) but with negative bias (-0.63 and -0.28, electronic supplementary material, figure S4).

(b) Community net production

(i) Mean rates per cell

Assuming a constant energy use per cell grossly overestimated community net production (figure 2*b*). This approach had the lowest precision (R^2 = 0.01 and 0.005), greatest bias (approx. 1), and lowest accuracy (RMSE approx. 30, electronic supplementary material, table S3).

(ii) Mean biomass-specific cell rates

The mean biomass-specific net production among species predicted changes in community production remarkalbly accurately, ranking second in both runs (RMSE = 1.10 and 1.03, figure 2*d*). This approach had good precision (R^2 = 0.52 and 0.55, electronic supplementary material, table S3) but positive bias especially for larger values (0.29 and 0.47; electronic supplementary material, figure S6).

(iii) Size-dependent cell rates across species

This approach was a poor predictor of the communtiy net production having low precision (0.08 and 0.37), high bias (0.82 and 0.61), and low accuracy (RMSE = 2.27 and 1.58, electronic supplementary material, table S3, figure 2*f*).

(iv) Size- and density-dependent cell rates across species

Accounting for the effects of both size and density across species improved predictions, to a greater extent when based on species densities (RMSE = 1.72 and 1.06, figure 2*h*) than on community density (electronic supplementary material, table S2, figure S5). However, this approach still had low precision (R^2 = 0.03 and 0.33) and positive bias (0.79 and 0.44, electronic supplementary material, table S3).

(v) Average individual species cell rates

Accounting for differences in energy use among species improved precision (R^2 = 0.55 and 0.45) but not bias (0.47 and 0.65, electronic supplementary material, table S3). This approach increased accuracy for run 1 (RMSE = 1.30), but decreased it for run 2 (RMSE = 1.59; figure 2j).

(vi) Density-dependent individual species cell rates

When accounting for density dependence, species rates were the best predictor of community net production when based on species densities (RMSE = 1, figure 2*l*). This approach had good precision (R^2 = 0.52 and 0.48), but positive bias (0.18 and 0.43) especially for larger values (electronic supplementary material, figure S6). Estimates based on community density were less accurate (electronic supplementary material, table S2, table S3) and underestimated community production (electronic supplementary material, figure S5).

(c) Why is biomass-specific energy flux not affected by changes in cell size?

Below, we report the results for run 1 but the same findings apply to run 2 (electronic supplementary material, table S4, figure S8). During succession, the average cell energy use among species in communities increased nearly isometrically with average cell size (slope = 1.1, 95% CI = 1.04, 1.16 for metabolism, figure 3*a*; 1.12, CI = 1.07, 1.18 for net production, electronic supplementary material, figure S7, table S4). Simultaneously, total cell abundance decreased with cell size with a negative isometric slope (−1.02, CI = −1.1, −0.94, figure 3*b*). The negative covariance between size and abundance was only visible at the level of the whole community, while there was no clear relationship within most species (electronic supplementary material, figure S9). The almost reciprocal size scaling of cell energy flux and abundance within communities meant that community energy flux was, at any point in time, nearly independent of average cell size (i.e. energy

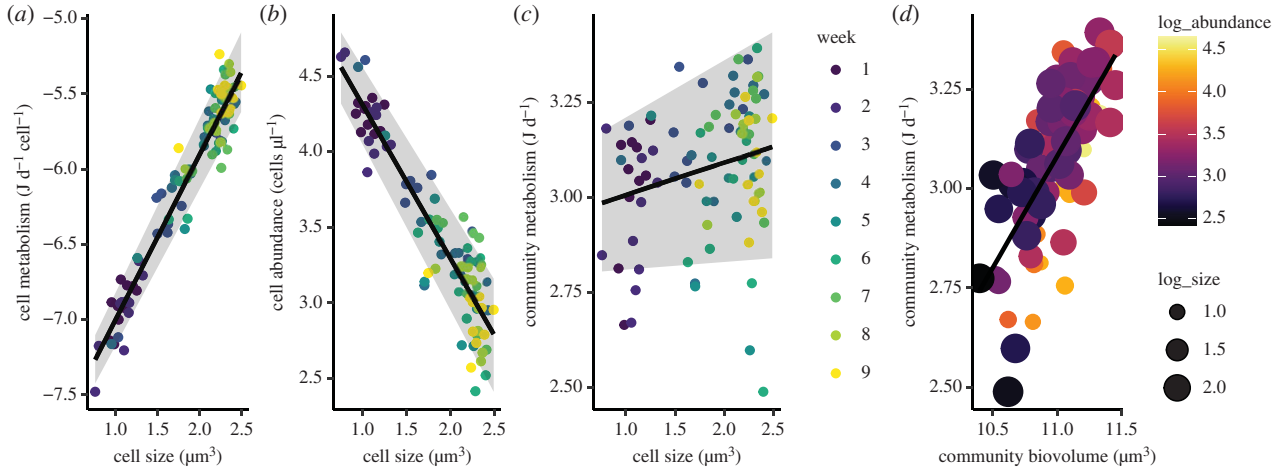

Figure 3. Over time, average cell metabolism (*a*) increased nearly isometrically with average cell size in communities, but total cell abundance declined with average size with an almost inverse slope (*b*). The reciprocal size scaling of cell energy flux and abundance means that total community energy flux is (almost) independent of mean cell size (*c*), and mostly driven by total biovolume (*d*). All data are $\log_{10}$-transformed. Here shown for metabolism in run 1, see electronic supplementary material, figure S7 for net production and electronic supplementary material, figure S8 for run 2. (Online version in colour.)

equivalence)—nearly because community energy flux slightly increased with cell size but this relationship was weak (slope = 0.08, CI = 0.02, 0.15 for metabolism, figure 3*c*; 0.1, CI = 0.04, 0.18 for net production, electronic supplementary material, figure S7). While communities might have approached carrying capacity towards the end of the experiment, energy equivalence occurred throughout succession even when total community biovolume was distant from equilibrium (electronic supplementary material, figure S10). Finally, because average cell energy use scaled nearly isometrically with average cell size, community energy flux was predominantly driven by total biovolume with no clear influence of size structure (slope = 0.56, CI = 0.44, 0.69 for metabolism, figure 3*d*; 0.61, CI = 0.48, 0.75 for net production, electronic supplementary material, figure S7).

4. Discussion

By comparing different approaches, we find that energy–size relationships among species are not the most accurate nor consistent predictor of community energy flux, at least at small scales. Phytoplankton communities underwent substantial changes in size structure over time, with average cell size increasing by an order of magnitude over 10 weeks [35]. Based on the allometric scaling of metabolism with size for these species [29], a community of larger cells should have a lower biomass-specific energy flux than a community of smaller cells (figure 4) [2,3]. Hence, we would have expected interspecific scaling relationships to explain a larger proportion of total energy flux and approaches not accounting for size structure to perform poorly (e.g. mean rates per cell or mean biomass-specific rates). Whereas interspecific scaling relationships explained a maximum of approximately 40% in variance in community energy flux, similarly to previous findings [2], and their performance varied markedly across tests. Accounting for density-dependent energy use only slightly improved the accuracy of interspecific relationships. Conversely, the simplistic approach based on biomass-specific rates was the most consistent and accurate overall. Hence, while body size is a strong predictor of individual energy use, interspecific scaling relationships based on size can be poor predictors of community functioning [8,22].

The relatively poor performance of interspecific scaling relationships could be partly attributed to differences in density dependence among species. Community rates were predicted very accurately and with little bias when cell energy use and its density dependence were parametrized for individual species, but poorly without density information. The importance of density effects on energy use might differ among systems or habitats because species-specific rates (without density) can sometimes be sufficient to estimate community energy flux [19,21,26]. Regardless, the potential application of approaches based on species-specific rates is limited because they require a lot of data. Estimates from biomass-specific rates were at least as good, providing a much simpler way to estimate community function and indicating no influence of size structure on total energy flux.

Surprisingly, we found energy equivalence at any point in time during succession. Energy equivalence predicts that the maximum number of organisms per unit area depends on their metabolic rate (hence size), therefore total energy flux should be independent of size [34]. While this prediction should apply at carrying capacity [2,21,31], which might be approached by some communities towards the end of the experiment, we find that it occurs throughout succession even when communities are not yet at steady state. The higher metabolism of larger cells that dominated over time was almost perfectly compensated for by their lower abundance. A similar metabolic compensation was observed in phytoplankton communities under warming [21]. In both cases, size-abundance trade-offs meant that community energy flux was not influenced by size structure.

Energy equivalence does not necessarily explain why community energy flux can be predicted from biomass alone. Energy equivalence occurs with any value of scaling exponents as long as they are reciprocal (e.g. ¾ and −¾). Whereas biomass-specific energy use is constant only under isometry (scaling of 1, figure 4) [26,31]. The isometry of energy flux in these communities may seem paradoxical given that energy use scales allometrically with size for these species when measured in isolation at constant density

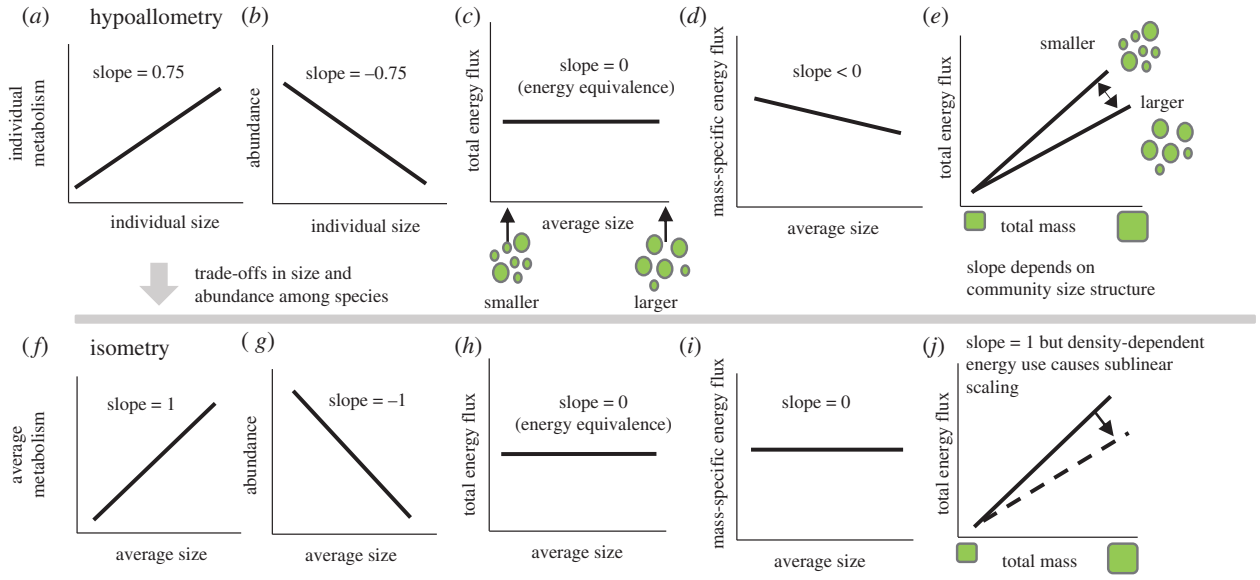

Figure 4. Diagram showing the consequences of hypoallometry ((*a*)–(*e*), any scaling less than 1) or isometry ((*f*)–(*j*)) for community energy flux in logarithmic space. Energy equivalence can occur in both cases but mass-specific energy use is independent of size only under isometry, where total energy flux is proportional to total biomass except where density-dependent effects cause sublinear scaling. (Online version in colour.)

[29]. But we show that size-abundance trade-offs among these species (of different size and energy use) cause the average energy use of cells in communities to scale isometrically with their average size. Species assembly can thus drive isometry of community energy flux, even if scaling is allometric for individual species [26].

The correlation between community energy flux and biovolume, however, broke down at high biovolumes dominated by large cells. Here, energy flux was consistently overestimated (electronic supplementary material, figure S11). While we can only speculate on this result, larger cells might be under stronger metabolic suppression where they dominate biomass [42]. A greater reduction in metabolic costs might allow larger species to sustain higher abundances and biovolumes than predicted from their size [8,32,43,44]. However, as biomass accumulates, community energy flux is overestimated if metabolic suppression is ignored. Indeed, while most approaches overestimated energy flux, this bias was lowest when we accounted for differences in density-dependent energy use among species. Metabolic reductions in response to competitors could thus explain the allometry of community production [26,45] and might become increasingly important as biomass accumulates.

While there is good evidence of metabolic suppression in response to conspecifics [27–29], the effects of heterospecifics remain largely unexplored [46]. By predicting cell energy use either as a function of species density (assuming only intraspecific competition) or community density (equal conspecific and heterospecific effects), we show that conspecifics are the main driver of metabolic suppression. However, metabolic suppression also occurs in response to heterospecifics but the strength of this response is weaker (electronic supplementary material, figures S4, S5), similarly to what competition theory predicts for resource use [47]. Whether the strength of heterospecific effects depends on their relative abundance remains to be explored.

While classic theory predicts that size drives energy flux and abundance [34], size and metabolism can concomitantly drive demography [15] complicating predictions for community energy flux. We show that trade-offs in size and abundance among species can alter the scaling of energy use with size in communities, so that community energy flux is predominantly driven by biomass alone (figure 4). This pattern occurs throughout succession even when communities are not at carrying capacity. Metabolic suppression in response to competitors can, however, constrain community energy flux causing sublinear scaling. Competitive effects on energy use have not been considered in detail, but our results suggest that they are important drivers of energy flux and need to be resolved to understand patterns of community function.

Data accessibility. Datasets are available at: https://doi.org/10.26180/5e30e9e2b02b3.

Authors' contributions. G.G. designed the study and collected data on phytoplankton communities; M.M. and D.J.M. performed the study on individual phytoplankton species. G.G. analysed the data and wrote the manuscript. All authors contributed to revisions.

Competing interests. We declare we have no competing interests.

Funding. G.G. and D.J.M. were supported by the Australian Research Council.

Acknowledgements. We are grateful to the handling editor and anonymous reviewers for their insightful comments. We also thank Belinda Comerford and Tormey Reimer for help with laboratory procedures.

References

1. Marquet PA, Quiñones RA, Abades S, Labra F, Tognelli M, Arim M, Rivadeneira M. 2005 Scaling and power-laws in ecological systems. *J. Exp. Biol.* **208**, 1749–1769. (doi:10.1242/jeb.01588)
2. Petchey OL, Long ZT, Morin PJ. 2007 The consequences of body size in model microbial ecosystems. In *Body size: the structure and function of aquatic ecosystems* (eds A Hildrew, D Raffelli, R Edmonds-Brown), pp. 245–265. Cambridge, UK: Cambridge University Press.
3. Perkins DM, McKie BG, Malmqvist B, Gilmour SG, Reiss J, Woodward G. 2010 Environmental warming and

biodiversity–ecosystem functioning in freshwater microcosms: partitioning the effects of species identity, richness and metabolism. In *Advances in ecological research* (ed. G Woodward), pp. 177–209. New York, NY: Academic Press.

4. Reuman DC *et al.* 2009 Allometry of body size and abundance in 166 food webs. In *Advances in ecological research*, pp. 1–44. New York, NY: Academic Press.
5. Andersen KH, Beyer JE. 2006 Asymptotic size determines species abundance in the marine size spectrum. *Am. Nat.* **168**, 54–61. (doi:10.1086/504849)
6. Carey N, Sigwart JD. 2014 Size matters: plasticity in metabolic scaling shows body-size may modulate responses to climate change. *Biol. Lett.* **10**, 8. (doi:10.1098/rsbl.2014.0408)
7. Yvon-Durocher G, Allen AP. 2012 Linking community size structure and ecosystem functioning using metabolic theory. *Phil. Trans. R. Soc. B Biol. Sci.* **367**, 2998–3007. (doi:10.1098/rstb.2012.0246)
8. Cyr H, Pace ML. 1993 Allometric theory: extrapolations from individuals to communities. *Ecology* **74**, 1234–1245. (doi:10.2307/1940493)
9. Enquist BJ. 2003 Scaling the macro ecological and evolutionary implications of size and metabolism within and across plant taxa. In *Macroecology: concepts and consequences, edition: 43rd symposium of the British Ecological Society (symposia of the British Ecological Society)* (eds TM Blackburn, KJ Gaston), pp. 321–341. Oxford, UK: Blackwell Publishing.
10. Schramski JR, Dell AI, Grady JM, Sibly RM, Brown JH. 2015 Metabolic theory predicts whole-ecosystem properties. *Proc. Natl Acad. Sci. USA* **112**, 2617–2622. (doi:10.1073/pnas.1423502112)
11. Perkins DM, Perna A, Adrian R, Cermeño P, Gaedke U, Huete-Ortega M, White EP, Yvon-Durocher G. 2019 Energetic equivalence underpins the size structure of tree and phytoplankton communities. *Nat. Commun.* **10**, 255. (doi:10.1038/s41467-018-08039-3)
12. Brown JH, Gillooly JF, Allen AP, Savage VM, West GB. 2004 Response to forum commentary on 'Toward a Metabolic Theory of Ecology'. *Ecology* **85**, 1818–1821. (doi:10.1890/03-0800)
13. Muller-Landau HC *et al.* 2006 Testing metabolic ecology theory for allometric scaling of tree size, growth and mortality in tropical forests. *Ecol. Lett.* **9**, 575–588. (doi:10.1111/j.1461-0248.2006.00904.x)
14. Brose U, Ehnes RB, Rall BC, Vucic-Pestic O, Berlow EL, Scheu S. 2008 Foraging theory predicts predator–prey energy fluxes. *J. Anim. Ecol.* **77**, 1072–1078. (doi:10.1111/j.1365-2656.2008.01408.x)
15. Malerba ME, Marshall DJ. 2019 Size-abundance rules? Evolution changes scaling relationships between size, metabolism and demography. *Ecol. Lett.* **22**, 1407–1416. (doi:10.1111/ele.13326)
16. Alcaraz M. 2016 Marine zooplankton and the metabolic theory of ecology: is it a predictive tool? *J. Plankton Res.* **38**, 762–770. (doi:10.1093/plankt/fbw012)
17. Price CA, Gilooly JF, Allen AP, Weitz JS, Niklas KJ. 2010 The metabolic theory of ecology: prospects and challenges for plant biology. *New Phytol.* **188**, 696–710. (doi:10.1111/j.1469-8137.2010.03442.x)
18. Cyr H, Pace ML. 1992 Grazing by zooplankton and its relationship to community structure. *Can. J. Fish. Aquat. Sci.* **49**, 1455–1465. (doi:10.1139/f92-160)
19. Zwart JA, Solomon CT, Jones SE. 2015 Phytoplankton traits predict ecosystem function in a global set of lakes. *Ecology* **96**, 2257–2264. (doi:10.1890/14-2102.1)
20. Dossena M, Yvon-Durocher G, Grey J, Montoya JM, Perkins DM, Trimmer M, Woodward G. 2012 Warming alters community size structure and ecosystem functioning. *Proc. R. Soc. B* **279**, 3011–3019. (doi:10.1098/rspb.2012.0394)
21. Padfield D, Buckling A, Warfield R, Lowe C, Yvon-Durocher G. 2018 Linking phytoplankton community metabolism to the individual size distribution. *Ecol. Lett.* **21**, 1152–1161. (doi:10.1111/ele.13082)
22. de Castro F, Gaedke U. 2008 The metabolism of lake plankton does not support the metabolic theory of ecology. *Oikos* **117**, 1218–1226. (doi:10.1111/j.2008.0030-1299.16547.x)
23. Rall BC, Kalinkat G, Ott D, Vucic-Pestic O, Brose U. 2011 Taxonomic versus allometric constraints on non-linear interaction strengths. *Oikos* **120**, 483–492. (doi:10.1111/j.1600-0706.2010.18860.x)
24. Glazier DS. 2005 Beyond the '3/4-power law': variation in the intra- and interspecific scaling of metabolic rate in animals. *Biol. Rev.* **80**, 611–662. (doi:10.1017/S1464793105006834)
25. Bokma F. 2004 Evidence against universal metabolic allometry. *Funct. Ecol.* **18**, 184–187. (doi:10.1111/j.0269-8463.2004.00817.x)
26. Ghedini G, White CR, Marshall DJ. 2018 Metabolic scaling across succession: do individual rates predict community-level energy use? *Funct. Ecol.* **32**, 1447–1456. (doi:10.1111/1365-2435.13103)
27. Ghedini G, White CR, Marshall DJ. 2017 Does energy flux predict density-dependence? An empirical field test. *Ecology* **98**, 3116–3126. (doi:10.1002/ecy.2033)
28. DeLong JP, Hanley TC, Vasseur DA. 2014 Competition and the density dependence of metabolic rates. *J. Anim. Ecol.* **83**, 51–58. (doi:10.1111/1365-2656.12065)
29. Malerba ME, White CR, Marshall DJ. 2017 Phytoplankton size-scaling of net-energy flux across light and biomass gradients. *Ecology* **98**, 3106–3115. (doi:10.1002/ecy.2032)
30. DeLong JP, Okie JG, Moses ME, Sibly RM, Brown JH. 2010 Shifts in metabolic scaling, production, and efficiency across major evolutionary transitions of life. *Proc. Natl Acad. Sci. USA* **107**, 12 941–12 945. (doi:10.1073/pnas.1007783107)
31. Huete-Ortega M, Cermeño P, Calvo-Díaz A, Marañón E. 2011 Isometric size-scaling of metabolic rate and the size abundance distribution of phytoplankton. *Proc. R. Soc. B* **279**, 1815–1823. (doi:10.1098/rspb.2011.2257)
32. Marañón E. 2015 Cell size as a key determinant of phytoplankton metabolism and community structure. *Ann. Rev. Mar. Sci.* **7**, 241–264. (doi:10.1146/annurev-marine-010814-015955)
33. Long ZT, Morin PJ. 2005 Effects of organism size and community composition on ecosystem functioning. *Ecol. Lett.* **8**, 1271–1282. (doi:10.1111/j.1461-0248.2005.00830.x)
34. Damuth J. 1981 Population-density and body size in mammals. *Nature* **290**, 699–700. (doi:10.1038/290699a0)
35. Ghedini G, Loreau M, Marshall DJ. 2020 Community efficiency during succession: a test of MacArthur's minimisation principle in phytoplankton communities. *Ecology* **101**, e03015. (doi:10.1002/ecy.3015)
36. Williams PJIB, Laurens LML. 2010 Microalgae as biodiesel & biomass feedstocks: review & analysis of the biochemistry, energetics & economics. *Energy Environ. Sci.* **3**, 554–590. (doi:10.1039/B924978H)
37. Brose U, Martinez ND, Williams RJ. 2003 Estimating species richness: sensitivity to sample coverage and insensitivity to spatial patterns. *Ecology* **84**, 2364–2377. (doi:10.1890/02-0558)
38. Walther BA, Moore JL. 2005 The concepts of bias, precision and accuracy, and their use in testing the performance of species richness estimators, with a literature review of estimator performance. *Ecography* **28**, 815–829. (doi:10.1111/j.2005.0906-7590.04112.x)
39. Bates D, Mächler M, Bolker B, Walker S. 2015 Fitting linear mixed-effects models using lme4. *J. Stat. Softw.* **67**, 48. (doi:10.18637/jss.v067.i01).
40. Kuznetsova A, Brockhoff PB, Christensen RHB. 2017 lmerTest Package: tests in linear mixed effects models. *J. Stat. Softw.* **82**, 26. (doi:10.18637/jss.v082.i13)
41. Fox J, Weisberg S. 2019 *An {R} companion to applied regression, third edition*. Thousand Oaks, CA: Sage. https://socialsciences.mcmaster.ca/jfox/Books/Companion/.
42. Henderson PA, Magurran AE. 2014 Direct evidence that density-dependent regulation underpins the temporal stability of abundant species in a diverse animal community. *Proc. R. Soc. Biol. Sci.* **281**, 20141336. (doi:10.1098/rspb.2014.1336)
43. Ulrich W, Hoste-Danyłow A, Faleńczyk-Koziróg K, Hajdamowicz I, Ilieva-Makulec K, Olejniczak I, Stańska M, Wytwer J. 2015 Temporal patterns of energy equivalence in temperate soil invertebrates. *Oecologia* **179**, 271–280. (doi:10.1007/s00442-015-3317-3)
44. Malerba ME, White CR, Marshall DJ. 2017 Eco-energetic consequences of evolutionary shifts in body size. *Ecol. Lett.* **21**, 54–62. (doi:10.1111/ele.12870)
45. Hatton IA, McCann KS, Fryxell JM, Davies TJ, Smerlak M, Sinclair ARE, Loreau M. 2015 The predator-prey power law: biomass scaling across terrestrial and aquatic biomes. *Science* **349**, 6252. (doi:10.1126/science.aac6284)
46. Janča M, Gvoždík L. 2017 Costly neighbours: heterospecific competitive interactions increase metabolic rates in dominant species. *Sci. Rep.* **7**, 5177. (doi:10.1038/s41598-017-05485-9)
47. Adler PB, Smull D, Beard KH, Choi RT, Furniss T, Kulmatiski A, Meiners JM, Tredennick AT, Veblen KE. 2018 Competition and coexistence in plant communities: intraspecific competition is stronger than interspecific competition. *Ecol. Lett.* **21**, 1319–1329. (doi:10.1111/ele.13098)